Available online at www.sciencedirect.com
ScienceDirect
Ceramics International 37 (2011) 1905–1909
CERAMICS INTERNATIONAL
www.elsevier.com/locate/ceramint

Structural and magnetic properties of $NiFe_{2-x}Bi_xO_4$ ($x = 0$, 0.1, 0.15) nanoparticles prepared via sol–gel method

Mohammad Javad Nasr Isfahani [a,*], Parisa Nasr Isfahani [b], Klebson Lucenildo Da Silva [c], Armin Feldhoff [d], Vladimir Šepelák [e]

[a] Islamic Azad University, Lenjan Branch, Isfahan, Iran
[b] Faculty of Chemistry, Isfahan University of Technology, Isfahan, Iran
[c] Department of Physics, State University of Maringá, Av. Colombo 5790, 87020-900 Maringá, Brazil
[d] Institute of Physical Chemistry and Electrochemistry, Leibniz University Hannover, Callinstr. 3-3A, 30167 Hannover, Germany
[e] Institute of Nanotechnology, Karlsruhe Institute of Technology, Herrmann-von-Helmholtz-Platz 1, 76344 Eggenstein-Leopoldshafen, Germany

Received 4 January 2011; received in revised form 8 February 2011; accepted 11 February 2011
Available online 19 February 2011

Abstract

$NiFe_{2-x}Bi_xO_4$ ($x = 0$, 0.1, 0.15) nanopowders were synthesized via sol–gel method. The precursor gels were calcined at 773 K in air for 1 h to obtain the pure nanostructured $NiFe_{2-x}Bi_xO_4$ spinel phase. The crystal structure and magnetic properties of the substituted spinel series of $NiFe_{2-x}Bi_xO_4$ have been investigated by means of ^{57}Fe Mössbauer spectroscopy, transmission electron microscopy and alternating gradient force magnetometry. Mössbauer spectroscopic measurements revealed that Bi^{3+} cations tend to occupy octahedral positions in the structure of the substituted ferrite, i.e., the crystal-chemical formula of the as-prepared nanoparticles may be written as: $(Fe)[NiFe_{1-x}Bi_x]O_4$ ($x = 0$, 0.1, 0.15), where parentheses and square brackets enclose cations on sites of tetrahedral and octahedral coordination, respectively. Selective area electron diffraction studies provided evidence that the samples of the $NiFe_{2-x}Bi_xO_4$ series, independently of x, exhibit the cubic spinel structure. The values of the saturation magnetization and the coercive field of $NiFe_{2-x}Bi_xO_4$ nanoparticles were found to decrease with increasing degree of bismuth substitution.

Keywords: D. Ferrite; Nanostructured materials; Sol–gel method; Mössbauer spectroscopy

1. Introduction

Nanosized spinel-type ferrites with the general formula MFe_2O_4 (M is a divalent metal cation) have attracted considerable attention during the past several decades [1]. Their unique properties, for instance, an enhanced chemical reactivity, an enhanced magnetization, and an enhanced magnetic ordering temperature [2–4], make them attractive, both from the scientific and application points of view. There are various techniques to obtain MFe_2O_4 nanoparticles such as hydrothermal reactions [5], coprecipitation [6], combustion synthesis [7], thermal decomposition [8], mechanosynthesis [9], microwave processing [10], electrospinning [11], the reverse micelle technique [12], the plasma deposition method [13], the radio-frequency thermal plasma torch technique [14], the pulsed wire discharge [15], sonochemical synthesis [16], and sol–gel method [17]. The latter method generally refers to the hydrolysis and the condensation of a metal nitrate or citrate, leading to dispersions of oxide particles in a ''sol''. The ''sol'' is then dried or ''gelled'' by the solvent removal or by a chemical reaction. The solvent used is generally water, but the precursors can also be hydrolyzed by an acid or base [18]. The rates of hydrolysis and condensation are important parameters that affect the particle size and, consequently, macroscopic properties of the final products. The particle size of a final nanooxide also depends on the solution composition, pH, and sintering temperature [19].

The particle size- and shape-dependent magnetic properties of MFe_2O_4 nanomaterials [20] can additionally be changed by the substitution of M^{2+} and/or Fe^{3+} cations. The system under

* Corresponding author. Tel.: +98 913 3195944; fax: +98 334 2432522.
E-mail address: nasr_phy@yahoo.com (M.J. Nasr Isfahani).

0272-8842/$36.00
doi:10.1016/j.ceramint.2011.02.003

the present investigation is bismuth-substituted nickel nanoferrite, $NiFe_{2-x}Bi_xO_4$ ($x = 0$, 0.1, 0.15), prepared via sol–gel method. Although a lot of work concerning the substituted nickel ferrites has already been published, see, e.g. [21,22], to the best of our knowledge, there is no report in the literature on the sol–gel prepared nanocrystalline $NiFe_{2-x}Bi_xO_4$. The effect of substitution of magnetic Fe^{3+} ions by diamagnetic Bi^{3+} cations on the structural and magnetic properties of the ferrite is investigated in the present fundamental study. Note that undoped nickel ferrite ($NiFe_2O_4$) is basically an inverse spinel ferrite, in which tetrahedral (A) sites are occupied by ferric ions, and octahedral [B] sites by ferric and divalent nickel ions; thus, the crystal-chemical formula of this compound can be represented as $(Fe^{3+})[Ni^{2+}Fe^{3+}]O_4$ [21].

2. Experimental

$NiFe_{2-x}Bi_xO_4$ ($x = 0$, 0.1, 0.15) nanopowders were prepared via sol–gel method. Stoichoimetric amounts of $Fe(NO_3)_3$, $Ni(NO_3)_2$ and $Bi(NO_3)_3$ were dissolved completely in deionized water. In the dissolving process, the ratio of cation concentrations of $Ni^{2+}/(Bi^{3+} + Fe^{3+})$ was fixed at 2 and that of $xBi^{3+}/(2 - x)Fe^{3+}$ was varied with $x = 0$, 0.1 and 0.15. Each aqueous solution containing Ni^{2+}, Fe^{3+} and Bi^{3+} was poured into citric acid with the ratio of $(Ni^{2+} + Bi^{3+} + Fe^{3+})$/(citric acid) = 3. The mixtures were stirred and slowly evaporated at 353 K to form gels. These gels were dried at 373 K for 2 h and then heated in air at 773 K for 1 h.

Mössbauer spectra were taken in transmission geometry at room temperature. A ^{57}Co/Rh γ-ray source was used. The velocity scale was calibrated relative to ^{57}Fe in Rh. Recoil spectral analysis software [23] was used for the quantitative evaluation of the Mössbauer spectra. Hysteresis loops of the as-prepared $NiFe_{2-x}Bi_xO_4$ ($x = 0$, 0.1, 0.15) samples were measured at room temperature using an alternating gradient force magnetometer (AGFM).

The morphology of powders was studied using a combined field-emission (scanning) transmission electron microscope (S)TEM (JOEL JEM-2100F) with an ultrahigh-resolution pole piece that provides a point resolution better than 0.19 nm at 200 kV. Prior to TEM investigations, powders were crushed in a mortar, dispersed in ethanol, and fixed on a copper-supported carbon grid.

3. Results and discussion

Room-temperature Mössbauer spectra of the as-prepared $NiFe_{2-x}Bi_xO_4$ ($x = 0$, 0.1, 0.15) samples are shown in Fig. 1. The spectrum of the $NiFe_{2-x}Bi_xO_4$ ($x = 0$) sample, presented in Fig. 1a, is well fitted with two subspectra with isomer shifts $IS_{(A)} = 0.12(1)$ mm/s and $IS_{[B]} = 0.23(3)$ mm/s characteristic of tetrahedrally (A) and octahedrally [B] coordinated Fe^{3+} cations in the spinel structure, respectively [24]. The intensities of the corresponding subspectra ($I_{(A)}$, $I_{[B]}$) with the hyperfine magnetic fields of $H_{(A)} = 48.01(5)$ T and $H_{[B]} = 51.54(4)$ T, revealed a fully inverse spinel structure of the ferrite with the degree of inversion of 1.00(1). Thus, based on the results of

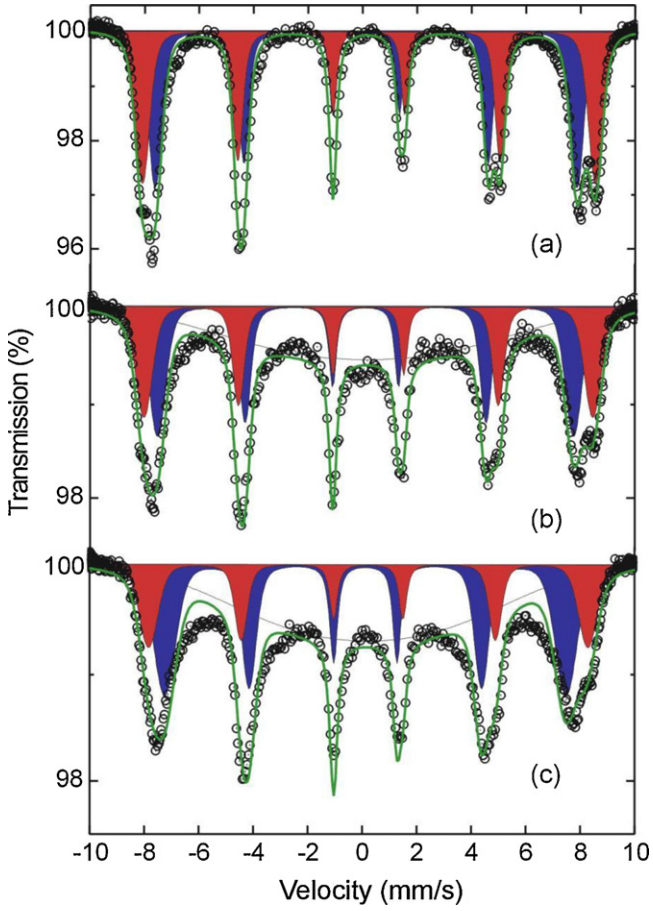

Fig. 1. Room-temperature ^{57}Fe Mössbauer spectra of $NiFe_{2-x}Bi_xO_4$ with various degree of substitution: (a) $x = 0$, (b) $x = 0.1$, (c) $x = 0.15$. Blue and red colours indicate subspectra corresponding to tetrahedrally (A) and octahedrally [B] coordinated Fe^{3+} cations, respectively. (For interpretation of the references to color in the text, the reader is referred to the web version of the article.)

Mössbauer analysis, the crystal-chemical formula of the as-prepared $NiFe_2O_4$ compound may be written as follows: $(Fe)[NiFe]O_4$. This finding is in agreement with previously published data on $NiFe_2O_4$ [25,26].

The typical feature of the Mössbauer spectra of the substituted $NiFe_{2-x}Bi_xO_4$ samples ($x = 0.1$, 0.15) is a 'sugging' background (see Fig. 1b and c); therefore, we had to introduce a broad, structureless background absorption to account for unresolved magnetic relaxation processes in a qualitative way (see, e.g., Refs. [27,28]). As clearly visible in Fig. 1, the relative intensity of the [B] subspectrum of the $NiFe_{2-x}Bi_xO_4$ samples

Table 1
The average magnetic hyperfine fields ($H_{(A)}$, $H_{[B]}$), the saturation magnetization (M_s) and the coercive field (H_c) of the as-prepared $NiFe_{2-x}Bi_xO_4$ nanoparticles with various x.

x	$H_{(A)}$ (T)	$H_{[B]}$ (T)	M_s (emu/g)	H_c (Oe)
0	48.01(5)	51.54(4)	42	100
0.1	47.37(1)	51.10(3)	35	40
0.15	45.67(7)	49.98(6)	29	25

decreases with increasing x. This can be interpreted as the substitution of Fe^{3+} ions by Bi^{3+} cations on [B] sites. Assuming that all the Bi^{3+} cations in the $NiFe_{2-x}Bi_xO_4$ samples are located on [B] sites, the degree of substitution, x_{calc}, can be determined from the Mössbauer subspectral intensities according to following expression: $I_{(A)}/I_{[B]} = 1/(1 - x_{calc})$. The calculated values $x_{calc} = 0.09(1)$ and $0.17(3)$ for $NiFe_{1.9}Bi_{0.1}O_4$ and $NiFe_{1.85}Bi_{0.15}O_4$ samples, respectively, are in agreement with the values of their ''real'' chemical substitution, i.e., $x = 0.1$ and 0.15. Thus, taking into account both, the present results of Mössbauer analysis and the strong preference of Ni^{2+} cations for octahedral coordination, the crystal-chemical formula of the substituted $NiFe_{2-x}Bi_xO_4$ samples may be written as $(Fe)[NiFe_{1-x}Bi_x]O_4$.

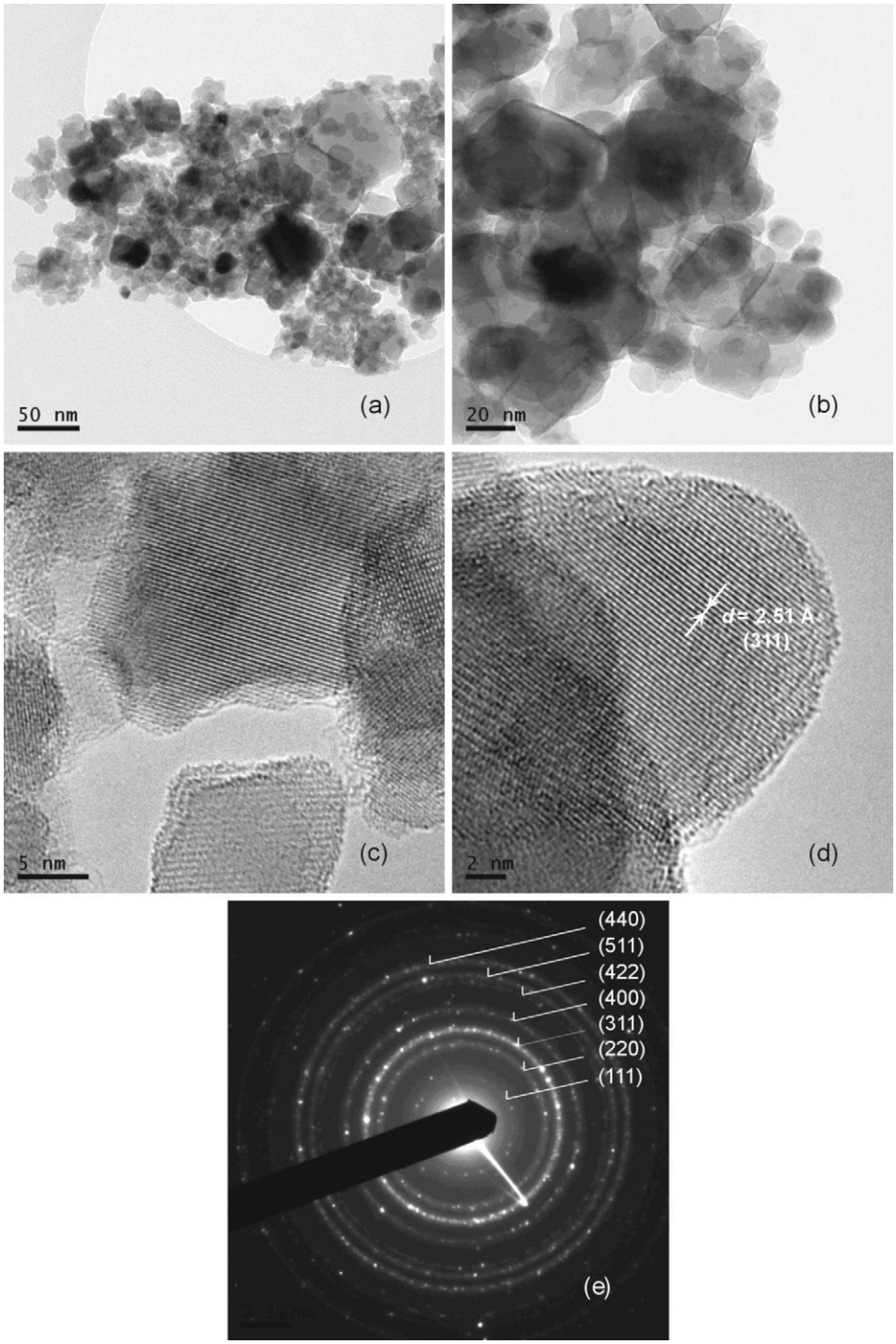

Fig. 2. (a) and (b) TEM bright-field images of $NiFe_{1.85}Bi_{0.15}O_4$ nanoparticles. (c) and (d) High-resolution TEM micrographs of $NiFe_{1.85}Bi_{0.15}O_4$ nanocrystals show the lattice fringes corresponding to the crystallographic planes (3 1 1) ($d = 2.51$ Å) of the spinel phase (JCPDS PDF 10-0325). (e) SAED pattern of $NiFe_{1.85}Bi_{0.15}O_4$ nanoparticles. Debye Scherrer rings, which fit to the cubic spinel structure, are denoted by Miller indices.

It was found that the hyperfine magnetic fields ($H_{(A)}$, $H_{[B]}$) acting on iron nuclei in (A) and [B] sublattices of $NiFe_{2-x}Bi_xO_4$ decrease with increasing degree of substitution x (see Table 1). This observation can be explained by the weakening of the (A)-O-[B] superexchange interaction due to the substitution of magnetic Fe^{3+} ions by diamagnetic Bi^{3+} cations on the [B] sites.

The morphology of the $NiFe_{2-x}Bi_xO_4$ ($x = 0$, 0.1, 0.15) samples was examined by direct observations via TEM. The representative bright-field TEM images (Fig. 2a and b) illustrate the nanoscale nature of the as-prepared $NiFe_{1.85}Bi_{0.15}O_4$ particles. As shown, the ferrite nanoparticles tend to agglomerate because they experience a permanent magnetic moment proportional to their volume [9]. Hence, each particle is permanently magnetized and gets agglomerated. The micrographs also show that the as-prepared ferrite consists of particles mostly in the 15–30 nm size range. The shape of the majority of the nanoparticles is found to be spherical. High-resolution TEM micrographs of nanocrystalline $NiFe_{1.85}Bi_{0.15}O_4$, presented in Fig. 2c and d, show lattice fringes corresponding to the crystallographic planes (3 1 1) ($d = 2.51$ Å) of the $NiFe_2O_4$ phase (JCPDS PDF 10-0325). The lattice fringes cross the whole volume of nanoparticles demonstrating their single-crystalline character.

It was found that the selected area electron diffraction (SAED) patterns of the $NiFe_{2-x}Bi_xO_4$ series, independently of x, consist of both the discrete diffraction spots and Debye–Scherrer rings characteristic of the spinel structure; see the representative SAED pattern of $NiFe_{1.85}Bi_{0.15}O_4$ displayed in Fig. 2e. These findings together with the results of Mössbauer investigations (Fig. 1) hint at the preservation of both the spinel structure and the valence state of iron cations in $NiFe_{2-x}Bi_xO_4$ with increasing x. Note that Debye Scherrer rings and the discrete diffraction spots in the SAED pattern, which fit to the cubic spinel structure, originate from the small particles and the well-crystalline regions of the larger grains of the as-prepared ferrite, respectively.

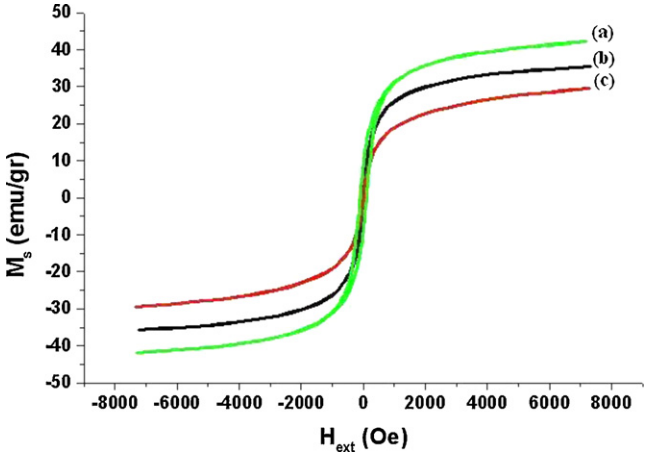

Fig. 3. The magnetization hysteresis loops recorded at room temperature for $NiFe_{2-x}Bi_xO_4$ nanoparticles with various degree of substitution: (a) $x = 0$, (b) $x = 0.1$, (c) $x = 0.15$.

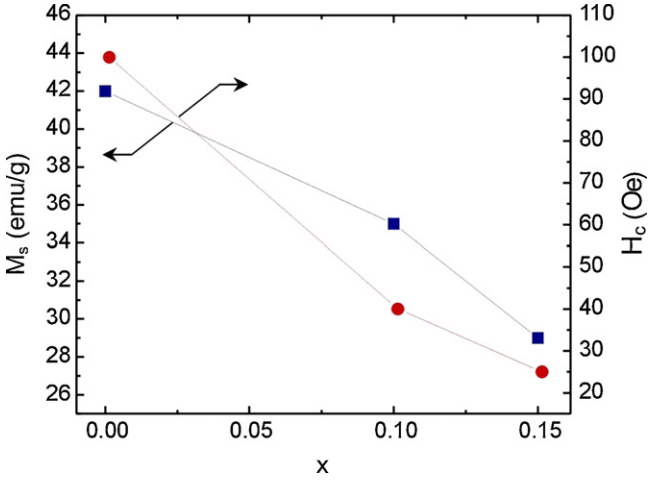

Fig. 4. The saturation magnetization (M_s) and coercive field (H_c) of nanosized $NiFe_{2-x}Bi_xO_4$ vs. x.

Fig. 3 shows the hysteresis curves for $NiFe_{2-x}Bi_xO_4$ ($x = 0$, 0.1, 0.15) nanoparticles. The measured values of the saturation magnetization (M_s) and of the coercive field (H_c) for all the samples are presented in Table 1 and Fig. 4, indicating the decrease of M_s and H_c with increasing Bi^{3+} concentration. Note that a very small hysteresis ($H_c = 25$ Oe) was observed for the as-prepared $NiFe_{1.85}Bi_{0.15}O_4$ nanoparticles indicating that the Bi-substituted nickel ferrite can be used most efficiently as a soft magnetic material with negligible hysteresis loss. The decrease of both the saturation magnetization and the coercivity with increasing x is explained as due to the magnetic dilution of the ferrite system by non-magnetic Bi^{3+} cations [21].

4. Conclusions

In this work, $NiFe_{2-x}Bi_xO_4$ ($x = 0$, 0.1, 0.15) nanoparticles were prepared for the first time via sol–gel method. ^{57}Fe Mössbauer and SAED measurements revealed the preservation of both the valence state of iron cations and the spinel structure of $NiFe_{2-x}Bi_xO_4$ series with increasing x. Due to the ability of Mössbauer spectroscopy to discriminate between probe nuclei on inequivalent crystallographic sites, valuable insight into the cation distribution in $NiFe_{2-x}Bi_xO_4$ is obtained. It is concluded that Bi^{3+} cations in the spinel $NiFe_{2-x}Bi_xO_4$ series occupy octahedral positions, i.e., the crystal-chemical formula of the substituted ferrites may be written as $(Fe)[NiFe_{1-x}Bi_x]O_4$. The substitution of Fe^{3+} cations by diamagnetic Bi^{3+} cations results in the reduction of both (A)- and [B]-site hyperfine magnetic fields. The experimentally determined M_s and H_c values of $NiFe_{2-x}Bi_xO_4$ are found to decrease monotonically with increasing degree of substitution x.

Acknowledgements

MJNI thanks the Iranian Nanotechnology Initiative for the support of this work. Partial support by the DFG is gratefully acknowledged.

References

[1] M.J. Nasr Isfahani, M. Myndyk, V. Šepelák, J. Amighian, A Mössbauer effect investigation of the formation of MnZn nanoferrite phase, J. Alloy Compd. 470 (2009) 434.

[2] V. Šepelák, U. Steinike, D.C. Uecker, R. Trettin, S. Wißmann, K.D. Becker, High-temperature reactivity of mechanosynthesized zinc ferrite, Solid State Ionics 101–103 (1997) 1343.

[3] V. Šepelák, A. Feldhoff, P. Heitjans, F. Krumeich, D. Menzel, F.J. Litterst, I. Bergmann, K.D. Becker, Nonequilibrium cation distribution, canted spin arrangement, and enhanced magnetization in nanosized $MgFe_2O_4$ prepared by a one-step mechanochemical route, Chem. Mater. 18 (2006) 3057.

[4] N. Ponpandian, A. Narayanasamy, C.N. Chinnasamy, N. Sivakumar, J.-M. Greneche, K. Chattopadhyay, K. Shinoda, B. Jeyadevan, K. Tohji, Neel temperature enhancement in nanostructured nickel zinc ferrite, Appl. Phys. Lett. 86 (2005) 192510.

[5] S. Komarneni, E. Fregeau, E. Breval, R. Roy, Hydrothermal preparation of ultrafine ferrites and their sintering, J. Am. Ceram. Soc. Commun. 71 (1988) C-26.

[6] F. Yazdani, M. Edrissi, Effect of pressure on the size of magnetite nanoparticles in the coprecipitation synthesis, Mater. Sci. Eng. B 171 (2010) 86.

[7] M.R. Barati, S.A. Seyyed Ebrahimi, A. Badiei, The role of surfactant in synthesis of magnetic nanocrystalline powder of $NiFe_2O_4$ by sol–gel auto-combustion method, J. Non-Cryst. Solids 354 (2008) 5184.

[8] F. Davar, M. Salavati-Niasari, N. Mir, K. Saberyan, M. Monemzadeh, E. Ahmadi, Thermal decomposition route for synthesis of Mn_3O_4 nanoparticles in presence of a novel precursor, Polyhedron 29 (2010) 1747.

[9] M.J. Nasr Isfahani, M. Myndyk, D. Menzel, A. Feldhoff, J. Amighian, V. Šepelák, Magnetic properties of nanostructured MnZn ferrite, J. Magn. Magn. Mater. 321 (2009) 152.

[10] S. Komarneni, M.C. D'Arrigo, C. Leonelli, G.C. Pellacani, H. Katsuki, Microwave-hydrothermal synthesis of nanophase ferrites, J. Am. Ceram. Soc. 81 (1998) 3041.

[11] A.M. Bazargan, S.M.A. Fateminia, M. Esmaeilpour Ganji, M.A. Bahrevar, Electrospinning preparation and characterization of cadmium oxide nanofibers, Chem. Eng. J. 155 (2009) 523.

[12] M.D. Shultz, M.J. Allsbrook, E.E. Carpenter, Control of the cation occupancies of MnZn ferrite synthesized via reverse micelles, J. Appl. Phys. 101 (2007) 09M518.

[13] M. De Marco, X.W. Wang, R.L. Snyder, J. Simmins, S. Bayya, M. White, M.J. Naughton, Mössbauer and magnetization studies of nickel ferrites, J. Appl. Phys. 73 (1993) 6287.

[14] S. Son, M. Taheri, E. Carpenter, V.G. Harris, M.E. McHenry, Synthesis of ferrite and nickel ferrite nanoparticles using radio-frequency thermal plasma torch, J. Appl. Phys. 91 (2002) 7589.

[15] P.Y. Lee, K. Ishizaka, H. Suematsu, W. Jiang, K. Yatsui, Magnetic and gas sensing property of nanosized $NiFe_2O_4$ powders synthesized by pulsed wire discharge, J. Nanopart. Res. 8 (2006) 29.

[16] A. Askarinejad, M. Bagherzadeh, A. Morsali, Catalytic performance of Mn_3O_4 and Co_3O_4 nanocrystals prepared by sonochemical method in epoxidation of styrene and cyclooctene, Mater. Lett. 62 (2008) 478.

[17] J. Azadmanjiri, H.K. Salehani, M.R. Barati, F. Farzan, Preparation and electromagnetic properties of $Ni_{1-x}Cu_xFe_2O_4$ nanoparticle ferrites by sol–gel auto-combustion method, Mater. Lett. 64 (2010) 1242.

[18] U.T. Lam, R. Mammucari, K. Suzuki, N.R. Foster, Processing of iron oxide nanoparticles by supercritical fluids, Ind. Eng. Chem. Res. 47 (2008) 599.

[19] A. Tavakoli, M. Sohrabi, A. Kargari, A review of methods for synthesis of nanostructured metals with emphasis on iron compounds, Chem. Pap. 61 (2007) 151.

[20] G. Salazar-Alvarez, J. Qin, V. Šepelák, I. Bergmann, I.M. Vasilakaki, K.N. Trohidou, J.D. Ardisson, W.A.A. Macedo, M. Mikhaylova, M. Muhammed, M.D. Baró, J. Nogués, Cubic versus spherical magnetic nanoparticles: The role of surface anisotropy, J. Am. Chem. Soc. 130 (2008) 13234.

[21] M.J. Nasr Isfahani, M. Myndyk, M. Eghbali Arani, J. Šubrt, V. Šepelák, Structural and Magnetic Properties of $NiFe_{2-2x}Sn_xCu_xO_4$, J. Magn. Magn. Mater. 322 (2010) 1744.

[22] M. Eghbali Arani, M.J. Nasr Isfahani, M. Almasi Kashi, Preparation and magnetic studies of nickel ferrite nanoparticles substituted by Sn^{4+} and Cu^{2+}, J. Magn. Magn. Mater. 322 (2010) 2944.

[23] K. Lagarec, D.G. Rancourt, Recoil–Mössbauer Spectral Analysis Software for Windows, version 1.02, Department of Physics, University of Ottawa, Ottawa, ON, 1998.

[24] F. Menil, Systematic trends of the ^{57}Fe Mössbauer isomer shifts in (FeO_n) and (FeF_n) polyhedra. Evidence of a new correlation between the isomer shift and the inductive effect of the competing bond T–X (→Fe) (where *X* is O or F and T any element with a formal positive charge), J. Phys. Chem. Solids 46 (1985) 763.

[25] V. Šepelák, D. Baabe, D. Mienert, D. Schultze, F. Krumeich, F.J. Litterst, K.D. Becker, Evolution of structure and magnetic properties with annealing temperature in nanoscale high-energy-milled nickel ferrite, J. Magn. Magn. Mater. 257 (2003) 377.

[26] V. Šepelák, I. Bergmann, A. Feldhoff, P. Heitjans, F. Krumeich, D. Menzel, F.J. Litterst, S.J. Campbell, K.D. Becker, Nanocrystalline nickel ferrite, $NiFe_2O_4$: mechanosynthesis, nonequilibrium cation distribution, canted spin arrangement, and magnetic behavior, J. Phys. Chem. C 111 (2007) 5026.

[27] M. Menzel, V. Šepelák, K.D. Becker, Mechanochemical reduction of nickel ferrite, Solid State Ionics 141–142 (2001) 663.

[28] J. Hesse, From FeNi-invar to reentrant spin-glasses, Hyperfine Interact. 47 (1989) 357.